



High-power modular LED-based illumination systems for mask-aligner lithography

JOHANA BERNASCONI,^{1,*} TORALF SCHARF,² UWE VOGLER,³ AND HANS PETER HERZIG¹

¹*Optics & Photonics Technology Laboratory, Ecole Polytechnique Fédérale de Lausanne (EPFL), Neuchâtel, 2002, Switzerland*

²*Nanophotonics and Metrology Laboratory, Ecole Polytechnique Fédérale de Lausanne (EPFL), Lausanne, 1015, Switzerland*

³*SUSS MicroOptics SA, Hauterive, 2068, Switzerland*

*johana.bernasconi@epfl.ch

Abstract: Mask-aligner lithography is traditionally performed using mercury arc lamps with wavelengths ranging from 250 nm to 600 nm with intensity peaks at the i, g and h lines. Since mercury arc lamps present several disadvantages, it is of interest to replace them with high power light emitting diodes (LEDs), which recently appeared on the market at those wavelengths. In this contribution, we present a prototype of an LED-based mask-aligner illumination. An optical characterization is made and the prototype is tested in a mask-aligner. Very good performances are demonstrated. The measured uniformity in the mask plane is 2.59 ± 0.24 % which is within the uniformity of the standard lamp. Print tests show resolution of 1 micron in contact printing and of 3 microns in proximity printing with a proximity gap of 30 microns.

© 2018 Optical Society of America under the terms of the [OSA Open Access Publishing Agreement](#)

OCIS codes: (220.0220) Optical design and fabrication; (220.2945) Illumination design; (220.3740) Lithography; (220.1770) Concentrators; (220.4880) Optomechanics; (220.4298) Nonimaging optics.

References and links

1. SUSS MicroTec datasheet <https://www.suss.com/en/products-solutions/mask-aligner>
2. R. S. West, "Side-emitting high-power LEDs and their application in illumination," *Proc. SPIE* **4776**, 171 (2002).
3. F. Fournier and J. Rolland, "Optimization of freeform lightpipes for light-emitting-diode projectors," *Appl. Opt.* **47**(7), 957–966 (2008).
4. B. Van Giel, Y. Meuret and H. Thienpont, "Using a fly's eye integrator in efficient illumination engines with multiple light-emitting diode light sources," *Opt. Eng.* **46**(4), 043001 (2007).
5. M. Erickstad, E. Gutierrez, and A. Groisman, "A low-cost low-maintenance ultraviolet lithography light source based on light-emitting diodes," *Lab Chip*, **15**(1), 57–61 (2015).
6. F. Y. Ciou, Y. C. Chen, C. T. Pan, P. H. Lin, P. H. Lin, and F. T. Hsu, "Investigation of uniformity field generated from freeform lens with UV LED exposure system," *Proc. SPIE* **9383**, 93830S (2015).
7. J. R. Sheats and B. W. Smith, *Microolithography: science and technology* (Marcel Dekker, 1998), Chap. 2.
8. O. Dross, R. Mohedano, M. Hernández, A. Cvetkovic, J. C. Miñano, and P. Benítez, "Koehler integrators embedded into illumination optics add functionality," *Proc. SPIE* **7103**, 71030G (2008).
9. P. Schreiber, S. Kudaev, P. Dannberg, and U. D. Zeitner, "Homogeneous LED-illumination using microlens arrays," *Proc. SPIE* **5942**, 188–196 (2005).
10. R. Voelkel, U. Vogler, A. Bich, P. Pernet, K. J. Weible, M. Hornung, R. Zoberbier, E. Cullmann, L. Stuerzebecher, T. Harzendorf and others, "Advanced mask aligner lithography: new illumination system," *Opt. Express* **18**(20), 20968–20978 (2010).
11. R. Winston, W. T. Welford, J. C. Miñano, and P. Benítez, *Nonimaging optics* (Elsevier Academic, 2005), Chap. 2.

1. Introduction

Mask-aligner lithography is a standard process used for the fabrication of structures in the micrometer range as used in technologies like MEMS, back-end semiconductor, micro-optics, photovoltaic, LED packaging, etc. In mask-aligner lithography, the illumination is very critical to make high-quality prints. The illumination in the mask plane needs to be as homogeneous

as possible, with values below 3 % uniformity [1]. The angular distribution of the radiation in the mask plane also has a big impact on the print quality and the intensity level determines the exposure time. Mask-aligner lithography in the spectral range of 350 to 450 nm is traditionally made with a mercury arc lamp illumination. But those light sources present several disadvantages which make them outdated: they are bulky; they are potentially dangerous because they contain mercury; they have a low electrical to optical power conversion efficiency with only about 1.5 to 5 % of the electrical power reaching the mask plane; they need a warm-up time of about 30 minutes and therefore cannot be switched on and off for each exposure; they have a low life-time, as the lamp light bulb has a lifetime of 1000 hours which is easily reached, because the lamp remains continuously on. In recent years, high-power LEDs in the required wavelength range appeared on the market, opening new doors to better illumination performances for mask-aligners. The advantages of LEDs for such an application are numerous. They have a lifetime which is much superior to the mercury arc lamp; they are easily switchable so can be switched on only when necessary. Other advantages are that they are safe, compact and do not require any maintenance. The main challenge is that a single LED does not have enough power.

Various examples of modeling and realizations of illumination systems based on LEDs can be found in literature, for lighting applications [2], projectors [3,4] or lithographic applications [5,6]. Here, a prototype of a modular LED-based optical system for mask-aligners is described. Where the application has similarities with what is presented by Erickstad et al. [5] the concept is more similar to what is theoretically presented by Van Giel et al. [4]; in our case a functional prototype is built and tested in practice. High power UV LEDs are used with optical reflectors in order to collect the light and homogenize the intensity. A high-power source can be formed by putting together multiple LED channels inside of individual reflectors. This forms a modular source which can easily be adapted to custom requirements. The source can directly be mounted into standard mask-aligners. A rigorous characterization is presented, which consists of an irradiance measurement of the light field, an angular distribution characterization (intensity measurement) as well as uniformity measurement. The LED-based system was mounted in a MA-BA8 Gen.3 SUSS mask-aligner in order to validate the prototype with print tests. The design of the system was supported by simulations with ray tracing (FRED).

2. Mask-aligner illumination

2.1. Mask-aligners with MO exposure optics

In general, in mask-aligner microlithography, the illumination consists of a lamp placed in a reflector to collect the light [7]. The collection is followed by different optical elements which act to shape the beam and transform the light source angular distribution and area into those required for the illumination. It is also at this stage that the homogenization of the light field is done. The illumination design of a mask-aligner with a specific beam shaping optics is shown in Fig. 1. The beam shaping optics is named MO Exposure Optics and it is used to obtain very good homogeneity levels of about $\pm 2.5\%$ ("contrast measurement", Eq. (4)). The mercury arc lamp is placed in the focal point of an ellipsoidal reflector, which collects the light from the different angles. The light is thus directed onto a first fly's eye integrator. Fly's eye integrators consist of two sets of microlenses arrays. Microlenses are widely used to homogenize the light field in illumination optics as presented by Dross et al. [8] and Schreiber et al. [9]. They divide the light into a multitude of channels, each one forming a secondary source. The space distribution of those secondary light sources is then turned into a flat-top angular distribution thanks to the first field lens (sometimes referred to as "Fourier lens"). The second field lens is placed to ensure collimation. The light then goes through another round of homogenization managed by the second fly's eye integrator, followed by a field lens converting the angular distribution to a flat-top pattern and the front lens ensuring telecentricity. The Illumination Filter Plate (IFP) is a shaped anodized aluminum plate. It is placed before the second integrator and makes it possible to shape

the angular distribution in the mask plane. The size of the light beam in this plane determines the angular extent in the mask plane, which is usually 1° to 3° . The working principle and advantages of such an illumination system are extensively detailed in the publication from Voelkel et al. [10].

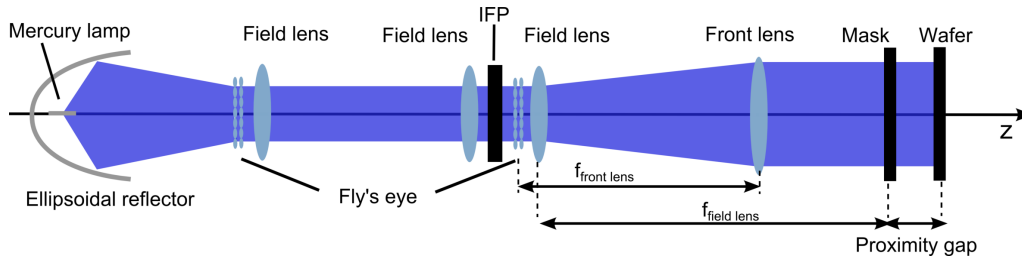


Fig. 1. Schematic of the illumination optics of a mask-aligner with MO Exposure Optics.

2.2. Mask-aligner illumination system with a stack of LEDs

The solution adopted for collecting the light from the LEDs is a set of individual reflectors, directly on top of the emitting surface of each LED. As shown in the schematic of Fig. 2, the light emitted with large angles can be brought within the acceptance angle of the fly's eye integrator. The angular distribution coming out of the reflectors is already homogenized going through the reflectors. This has the advantage of allowing the removal of the first set of integrator and its two field lenses, if correctly designed. The last part of the setup of Fig. 2 is the same as in Fig. 1.

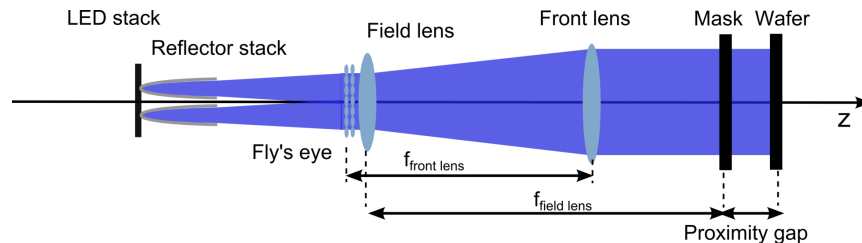


Fig. 2. Schematic of the illumination optics of a mask-aligner when replacing the mercury arc lamp with an array of LEDs and reflectors.

The light field on the fly's eye integrator of Fig. 2 determines the angular distribution in the mask plane. The reflectors array must therefore have the same size as the beam in the standard system, which matches the size of the fly's eye integrator. By choosing which LED to switch on, the angular distribution in the mask plane can be modified. The IFP can thus be removed and customized angular distributions can still be created. The resulting angular distribution in the mask-plane is slightly different from the one obtained with a standard system. The angular distribution with the array of reflectors is close to a piecewise flat-top, where the arc lamp and its optics give a continuous spectrum with a maximum for small angles and a decay towards larger angles. There is more power in the larger angles with the reflectors array, which might be interesting for high resolution prints.

In the end, the stack of LEDs and their reflectors can replace the mercury arc lamp and its ellipsoidal reflector, the first integrator, the two subsequent lenses and the IFP. The rest of the setup can remain unchanged, allowing an easy integration of the new system.

3. Design of the reflector

3.1. Optical design

The main challenge, when designing an illumination system, is to transform the size and angular distribution of a given light source into an illuminated area and angular extent which correspond to the requirements. In general, this conversion is ruled by the law of Etendue [11]. Considering a beam of radiation of cross section S and solid angle Ω , the Etendue is the integral over S and Ω , of the product of an element of surface with an element of direction cosine solid angle. This can be written as in Eq. (1) [11]. In an optical system, the Etendue is globally conserved. If there are aberrations, diffractive elements or microlenses, the Etendue can increase.

$$E = n^2 \int_S \int_{\Omega} dx dy dL dM \quad (1)$$

where dx , dy are small increments in position, dL , dM are small increments of direction cosine solid angle with respect to x , y .

The reflector is based on a parabolic compound concentrator, which is known to be used for solar applications [11]. Instead of being used as a collector, it is here thought as an illuminator. The source is placed in the entrance aperture of size $2a$, and the output is a light distribution within the angular extent defined by the geometry of the reflector. The surface reflecting the rays can be described by a parametric equation, given by Eq. (2) [11], with the use of the cylindrical coordinates, as shown in Fig. 3 and with a and a' being respectively the radius of the input and output apertures and θ_{max} the angular extent at the output of the reflector.

$$r = \frac{2f \sin(\phi - \theta_{max})}{1 - \cos \phi} - a, \quad z = \frac{2f \cos(\phi - \theta_{max})}{1 - \cos \phi}, \quad f = a(1 + \sin \theta_{max}) \quad (2)$$

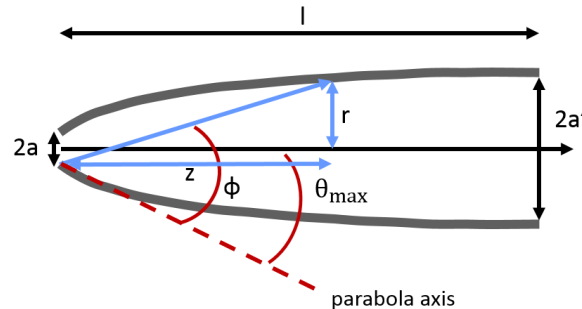


Fig. 3. Schematic of the parabolic compound concentrator.

The output aperture size and length of the reflector are both determined by the entrance aperture, the angular extent needed at the output and the conservation of Etendue. They are related by Eq. (3) [11]. In our case, the LEDs emit light within $\pm 60^\circ$ and the entrance aperture is given by the size of the emitting area of the LED, which is of $1.5 \times 1.5 \text{ mm}^2$; the angle θ_{max} is given by the acceptance angle of the fly's eye integrator, which is $\pm 10^\circ$; this two constrains result in an output aperture of 8.6 mm and a length of 28.7 mm.

$$l = \frac{a(1 + \sin \theta_{max}) \cos \theta_{max}}{\sin^2 \theta_{max}}, \quad a' = \frac{a}{\sin \theta_{max}} \quad (3)$$

Thanks to the optical design, a first estimation of the power efficiency of the reflectors can be done according to the number of reflections that the rays encounter. As the surface of the reflectors have a determined specular reflectance, it will determine the best achievable power efficiency for those reflectors. In our case, the measured specular reflectance of a simple polished aluminum sample without coating is about $66 \pm 5 \%$ at 400 nm. The error is found by repeating the measurement over different polished samples. According to simulation, most of the rays will undergo 0,1,2 or 3 reflections. In Table 3.1, the first column indicates the number of reflections which the rays undergo. The second column is the percentage of the source power it represents; in the case of the LED, 3 % of the source power undergo 0 reflections, which corresponds to direct light from the LED, 27 % undergo 1 reflections, etc. The majority of the light is reflected 2 times. The last column of the table represents the percentage of the initial source power which makes it to the output of the reflector with a specular reflectance of $66 \pm 5 \%$. In total, $46 \pm 6 \%$ of the initial power makes it to the output of the reflector, with most of the power coming from rays undergoing 1 or 2 reflections. The polishing of the surfaces has a important impact, as by improving it to reach 75 % of specular reflectance, the efficiency of the reflectors would go up to 57 %.

Table 1. Power efficiency with a specular reflectance of 66 %

Number of reflections	Source power [%]	Source power after reflections [%]
0	3	3
1	27	18
2	46	20
3	15	5
4	9	2
total	100	46

This evaluation allows the computation of a first estimation of the efficiency achievable with such a system. The collection efficiency from the LED to the reflector is estimated to be 80 %. The rest of the optics, which has an anti-reflective coating, is taken to have a total efficiency of 90 %, taking into account reflection and absorption losses. This adds up to an overall optical efficiency of 33 %. As the electrical to optical power efficiency of the LEDs are given to be about 25 % by the manufacturer, it means that the overall electrical to optical power efficiency of the system is estimated to be of 8 % with the current specular reflectance. This is 2-5 times better than the existing optical system with mercury arc lamp in mask-aligners.

3.2. Mechanical design

The mechanical design plays an important role in the overall efficiency of the illumination device. The challenge is to have the highest power density possible while considering the size of the LED. The emitting area of an LED has a finite size, which is smaller than the overall packaging size of the LED. Furthermore, each LED has to be wired electronically, which also adds up to the space required. The solution chosen consists in manufacturing one reflector for each LED, while making sure the entrance of the reflector fits perfectly to the emitting area of the LEDs. By putting an individual reflector for each LED, the space between each emitting area is used in an efficient way. The main challenge to build a prototype of a reflector, is the machining. Indeed, depending on the required angular distribution and entrance area, the reflector can become very long. In order to make it easy to manufacture and scalable, the reflectors consist of one unitary

piece, which we call “fan”, that is repeatedly assembled together. Four fans form a whole reflector, but each fan can be used for two reflectors as both sides are functional. This makes it very easy to build modules of different overall power. From a fabrication point of view, it is also of interest to have only one piece to replicate. A photography of a fan is shown in Fig. 4. The piece is symmetrical and both curved faces are the active surfaces. It is machined by CNC in aluminum and the active surfaces are polished to increase the specular reflectance.

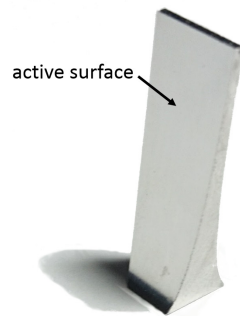


Fig. 4. Fan used to form the reflectors. The two symmetrical active surfaces are polished.

In Fig. 5, the assembly of four reflectors is shown. The LEDs are mounted on an aluminum PCB and a spacer is inserted between the reflector base and the PCB to allow space for the LED. The result is a very compact, modular design, which has also the advantage of being easily scalable. The fact that individual reflectors are used is crucial. One large reflector including all of the LEDs would not provide an irradiance high enough at the output of the reflector, and would be useless for this high-power application. The mechanics is therefore a key aspect and its fabrication is only made possible by the innovative mechanical design.

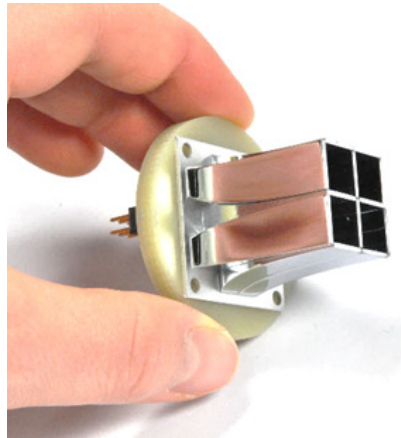


Fig. 5. Mechanical design of the reflector. Notice the repeated fan.

Table 3.2 illustrates the scalability of an LEDs module and the obtainable power. The optical power corresponds to what is given by the datasheet of the LED. It is 1.4 W at 405 nm and 1.03 at 365 nm, but for the sake of simplification, 1 W is taken. The power in the mask plane is given by the number of LEDs multiplied by 0.3, the efficiency of the system, which is described in the last paragraph of section 3.1. The last column gives the resulting irradiance in the mask plane

for a 8 inches by 8 inches (20.32x20.32 mm²) area. For comparison, a MA-BA8 Gen.3 SUSS mask-aligner which we have at our facilities, with a mercury arc lamp of 350 W electrical power gives, at 365nm (with the i-line filter), an irradiance of 7 mW/cm² and in broadband 30 mW/cm². This means that, in order to compare with such a lamp, a 4x4 module would be needed for 365 nm and a 7x7 module for broadband illumination. For broadband, modules at a different wavelength can also be combined with a dichroic mirror. A 7x7 module is also the size required in order to have a light beam of the size of the fly's eye integrator. The realization of such modules is realistic, providing that a heat management is included.

Table 2. Expected irradiance for LEDs module of different sizes

Module size	Optical power [W]	Power in the mask plane [W]	Irradiance in the mask plane [mW/cm ²]
1 LED	1	0.3	0.7
2x2 LEDs	4	1.2	2.9
4x4 LEDs	16	4.8	11.6
7x7 LEDs	49	14.7	35.6

The 2x2 module of Fig. 5 is used for further optical characterization. As the prototype does not include a heatsink, the LED cannot be driven at their maximum power. The optical power reached is only a fraction of what is actually needed in a mask-aligner, but such a prototype is necessary to validate the concept and the working principle of the device.

4. Characterization and performances of the prototype

The characterization process consists of different parts. The characterization of the irradiance after the reflector, the angular distribution measurement after the reflector, and the power efficiency of the reflector are first determined. The performances of the reflector illumination system has then to be validated with the rest of the optical system of a mask-aligner. Both irradiance homogeneity and prints test are performed to compare the performances in the machine with those of a mercury arc lamp. For all the homogeneity measurement, the uniformity is defined as the contrast of the resulting light field, and is computed according to the following equation:

$$U = \frac{I_{max} - I_{min}}{I_{max} + I_{min}} \quad (4)$$

4.1. Reflector characterization

In order to measure the irradiance, a two dimensional scanner is used to measure the light field in the x-y plane. A photodiode is mounted on two linear stages, which are controlled through Labview. A pinhole is placed in front of the photodiode to increase the resolution of the scans. The motors have a resolution of 1 μm in full step, therefore it is the pinhole which determines the resolution of the measurement. According to the sensitivity of the photodiode used, a pinhole down to the size of 200 μm can be used. For most of the characterization, though, a large surface has to be scanned and therefore an aperture size of 1 mm is chosen to reduce the scanning time. The irradiance at the output of the reflectors is shown in Fig. 6.

A similar setup is used for the angular characterization but the photodiode is mounted on two rotational scanners. The source is placed in the center of the rotation axis. Angular steps of

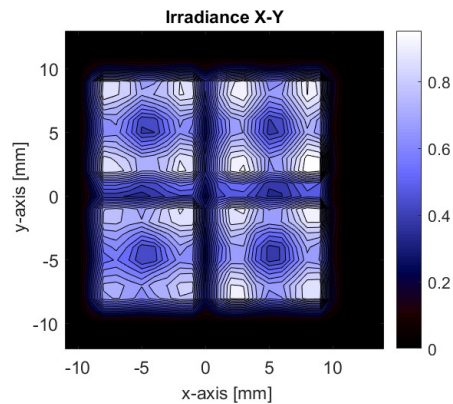


Fig. 6. Irradiance distribution at the output of the reflectors. Each channel can be identified as there is lost space between the channels.

0.5 degree are made to acquire the whole angular distribution. This allows the measurement of the intensity's homogeneity achieved by the different components. Figure 7 shows the angular distribution at the output of a single reflector. The levels on the image are set every 5%. The reflectors show an angular homogeneity within $\pm 4\%$.

The power efficiency is measured with a powermeter. The optical power at the output of the reflectors is measured and it is compared with the expected values from the datasheet according to the electrical power. The power measurement of the system showed an efficiency of the reflectors of $36 \pm 3\%$. According to the measured specular reflectance of the surface of the fans, which is $66 \pm 5\%$, the maximum efficiency is $46 \pm 6\%$. This was evaluated thanks to the number of reflection of the rays. The rest of the losses are due to collection efficiency at the source itself, with part of the light not entering the reflectors, and losses at the junction between two fans, where they superpose. This efficiency can be greatly improved by working on making an even better polishing, and by limiting the losses at the junctions with tighter tolerances.

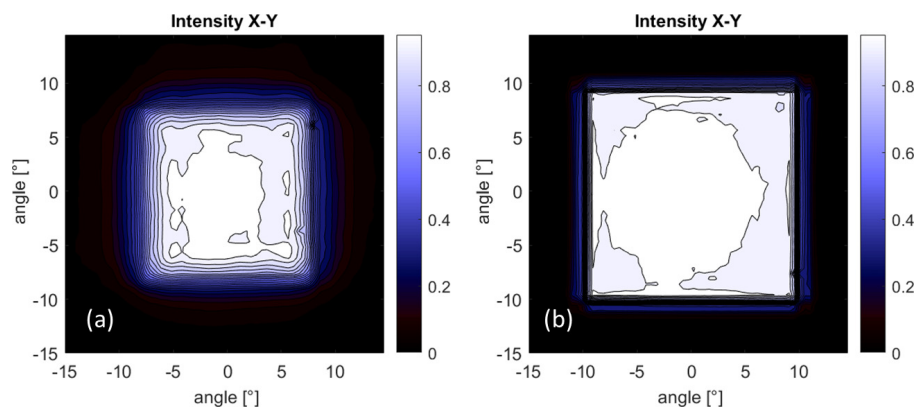


Fig. 7. (a) Intensity distribution after one reflector. The angles are contained within $\pm 10^\circ$. The uniformity is within $\pm 5\%$ (b) Intensity distribution after the reflectors and the Fly's eye integrator. The angular extent is $\pm 10^\circ$ and the uniformity is within $\pm 3\%$.

4.2. Field uniformity in the mask plane

In order to measure the performances under real conditions, the LEDs with the reflectors are mounted in a MA-BA8 Gen. 3 SUSS mask-aligner. They are placed at a distance of about 2 cm from the fly's eye integrator, as shown in the schematic of Fig. 2. The LEDs were not driven at their maximum power in order to avoid overheating, as the system does not include a heatsink.

First, a verification of the field uniformity respecting the standard procedure has to be done. To do so, a calibrated intensity-meter from SUSS is used in the mask plane to measure the intensity at different points of the illuminated area. The uniformity is then computed as a contrast, according to Eq.(4). A reference value was first measured with the mercury arc lamp over thirteen points over an 8 inches diameter surface. Different configurations were measured and the results are presented in Table 4.2. For the mask-aligner in broadband mode, the uniformity was found to be of $\pm 2.45 \pm 0.5$ %. This value corresponds to the specifications given by the company. When adding the i-line filter, the uniformity decreases to $\pm 2.9 \pm 1$ %. In comparison, the LED module gives a uniformity of $\pm 2.59 \pm 0.24$ %. This uniformity can probably still be improved when passing to a bigger system, which will result in more microlenses being illuminated.

Table 3. Summary of the uniformity measurements

Light source	Configuration	Mean Irradiance [mW/cm ²]	Uniformity [%]
350W Lamp	broadband	30	2.45 ± 0.5
350W Lamp	i-line (365nm)	7	2.9 ± 1
LED module	400nm	0.6	2.59 ± 0.24

4.3. Print tests

The ultimate test was to make prints with a test mask, with the LEDs system in the mask-aligner. The LEDs and reflectors system was mounted, like previously, just before the fly's eye integrator of a MA-BA8 Gen. 3 SUSS mask-aligner. Structures of different sizes ranging from 800 nm to tens of microns are present on the mask. Both contact printing and proximity printing, with a proximity gap set to 30 μm were carried out. A layer of 1 μm of AZ1518 resist was deposited on 4 inches silicon wafers. The wafer was then exposed to a dose of 44 mJ/cm², which was determined by doing a dose test. The development was done for 1 minute in AZ351B 4/1 from AZ Electronic Materials. In Fig. 8, the results are shown for both contact printing (a) and (b) and proximity printing (c) and (d). We can see that in contact, a resolution of 1 μm is achieved. This result was consistently repeated on different areas of the wafer. For the case with a 30 μm proximity gap, a resolution of 3 μm is achieved, but with strong diffraction effects. The diffraction effects are expected because of the small angles of incidence in the mask plane, which are below 1°. The 5 μm structures are well printed. Those results correspond to the expected printing resolutions.

5. Conclusion

A prototype of an LED-based system is demonstrated as replacement for a mercury arc lamp in mask-aligners. A system of 2x2 LEDs was built to first demonstrate the performances. This module consists in an assembly of individual fans mounted together. This allows to have a modular system which can easily be scaled. The prototype showed very good performances. The angular distribution after the reflectors demonstrated an intensity uniformity of ± 5 %. The distribution shows that most of the light is within an angular extent of $\pm 10^\circ$, which corresponds to the acceptance angle of the fly's eye integrator. The measurement after the microlenses shows

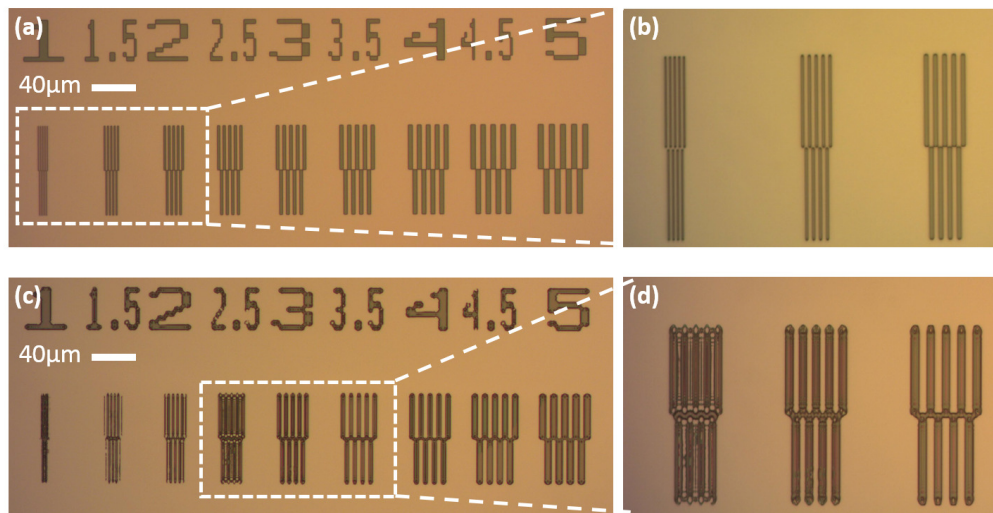


Fig. 8. Print test results in (a) and (b) contact printing and (c) and (d) in proximity printing with a proximity gap of 30 μm .

that the uniformity is within $\pm 4\%$, which corresponds to the datasheet of the element used for this characterization. The measured optical power efficiency of the reflectors is $36 \pm 3\%$. This efficiency can be improved by improving the polishing, choosing a better suited aluminum or applying a coating on the reflective surface. By setting the prototype in a MA-BA8 Gen. 3 mask-aligner, an uniformity of $\pm 2.59 \pm 0.24\%$ was found, which is as good as the performance with the mercury arc lamp. Print tests in contact and with 30 μm proximity gap were realized and resulted in respectively $< 1\ \mu\text{m}$ and 3 μm resolution, which, once again, corresponds to the specifications of the machine.

Funding

Kommission für Technologie und Innovation (KTI) (18188); Horizon 2020 Framework Programme (675745).

Acknowledgments

The authors acknowledge Marcel Groccia for the electronics, Irène Philippoussis for the help with the print tests, Raoul Kirner and Wilfried Noell from SUSS MicroOptics SA for interesting discussions about the system and its performances.

Disclosures

The authors declare that there are no conflicts of interest related to this article.